Liquid Crystals
Publication details, including instructions for authors and subscription information:
http://www.informaworld.com/smpp/title~content=t713926090

Bifurcational analysis of the isotropic-discotic nematic phase transition in the presence of extensional flow

Alejandro D. Rey[a]
[a] Department of Chemical Engineering, McGill University, Montreal, Canada

To cite this Article Rey, Alejandro D.(1995) 'Bifurcational analysis of the isotropic-discotic nematic phase transition in the presence of extensional flow', Liquid Crystals, 19: 3, 325 — 331
To link to this Article: DOI: 10.1080/02678299508031988
URL: http://dx.doi.org/10.1080/02678299508031988

LIQUID CRYSTALS, 1995, VOL. 19, NO. 3, 325–331

Bifurcational analysis of the isotropic–discotic nematic phase transition in the presence of extensional flow

by ALEJANDRO D. REY
Department of Chemical Engineering, McGill University, Montreal, Quebec H3A2A7, Canada

(*Received 30 January 1995; accepted 14 February 1995*)

A bifurcational analysis is performed on a version of Doi's equation of nematodynamics that describes the non-equilibrium isotropic–discotic nematic phase transition in the presence of steady uniaxial extensional flow. The disc-like molecular geometry and the degenerate extensional flow-induced orientation are shown to be the source of a complex bifurcation and multistability behaviour involving two physically equivalent biaxial nematic phases, one uniaxial nematic phase and one uniaxial paranematic phase. Depending on the temperature and the extension rate, the isotropic–discotic nematic transition, involving the two biaxial nematic phases and the uniaxial paranematic phase, may be continuous (2nd order), discontinuous (1st order), or it may exhibit a tricritical non-equilibrium phase transition point. A validation procedure on the validity of the predictions is implemented. The predictions presented here find practical applications in the industrial spinning of mesophase carbon fibres, and also provide new results that increase the present fundamental understanding of the rheology of discotic nematic liquid crystals.

1. Introduction

The objective of this paper is to present a bifurcational analysis and to provide a physical interpretation of the non-equilibrium isotropic–discotic nematic [1, 2] phase transition in the presence of steady, incompressible, isothermal, uniaxial extensional flow, using the well-known Doi theory of nematodynamics.

The practical significance of the phenomena reported in this paper is found in the manufacturing of mesophase carbon fibres, which is an industrial process that essentially consists of subjecting a biphasic isotropic–discotic nematic polydisperse mixture to a uniaxial extensional flow [3], and whose optimal design and control requires a basic understanding of the non-equilibrium isotropic–discotic nematic phase transition. The scientific significance of the presented predictions is to increase the current poor understanding of the rheology and flow behaviour of discotic nematic liquid crystals. Considerable theoretical and experimental efforts are being directed towards these newer classes of liquid crystals [2]. For the chemical structure of typical and existing thermotropic discotic nematics which may exhibit the phenomena reported in this paper we refer the reader to [2].

The equilibrium thermodynamic phase behaviour of the model nematic discotic liquid crystal adopted in this paper is given by the standard uniaxial Landau–de Gennes model [1]. In the absence of flow, and below a certain temperature, the model thermotropic material admits two stable uniaxial discotic nematic liquid crystalline phases; one is characterized by the ordering of the normal directions to the molecular discs along an axis of cylindrical symmetry, denoted by a unit vector **n**, called the director [1] (see figure 1), and the other by the ordering of the molecular normals away from **n**; the different order is captured by the sign of the scalar order parameter S, when $S > 0$ ($S < 0$) alignment is towards (away from) **n**. At a higher temperature range, the model discotic exhibits multistability, and admits a stable isotropic phase and the uniaxial discotic nematic phase with $S > 0$. Above a

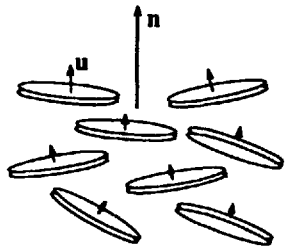

Figure 1. Schematic of a typical uniaxial discotic nematic liquid crystal ($S > 0$). The molecular geometry is approximated by circular discs. For discotic (rod-like) nematics the distinct direction is along (normal to) the shortest molecular dimension. The molecular unit normals (**u**) align preferentially along the average orientation or director (**n**). The uniaxial nematic phase has orientational order with cylindrical symmetry and positional disorder.

0267–8292/95 $10·00

certain transition temperature the isotropic phase is the only stable phase. In this paper we perform a mean field characterization of the main extensional flow effects on the multistability temperature range, and on the symmetry breakings of the molecular orientational order, neglecting fluctuation effects.

Figure 1 shows a schematic of the uniaxial discotic nematic phase for $0 < S < 1$; note that (i) the unit molecular normals ($\mathbf{u}$) are partially oriented along the average orientation $\mathbf{n}$; (ii) the projection of the molecular normals on a plane normal of $\mathbf{n}$ is isotropic, that is, there is equal likelihood of finding a projected $\mathbf{u}$ anywhere on the plane normal $\mathbf{u}$; (iii) for uniaxial discotic (rod-like) nematics the unique direction is along the shortest (longest) molecular dimension, a simple geometric fact that has been shown to starkly differentiate the rheological, optical, and electro-magnetic behaviour of discotic nematics from rod-like nematics [2]. Here we show that these drastic differences between rod-like and disc-like nematics are also reflected in the non-equilibrium isotropic–nematic phase transition under extensional flow.

The non-equilibrium isotropic–nematic phase transition of rod-like molecules has been extensively studied for shear [4–6] and elongational (potential) flows [6–8]. Predictions and observations for lyotropics and thermotropics show that the imposition of flow tends to shift the isotropic–nematic multistability gap to higher (lower) temperatures (concentrations), and that increasing the deformation rate shrinks the multistability gap to a critical point. In the phase plane the multistability region corresponds to temperature and deformation rate values for which the nematic and paranematic phases are linearly stable. In addition, for elongation flow [6] it was found that the average orientation is along the extension direction and that the nematic and paranematic phases remain uniaxial since the plane normal to $\mathbf{n}$ is subjected to a uniform isotropic compression.

In what follows we show that the extensional flow of fluids with disc-like molecules gives rise to a rich phenomenology of symmetry breakings and multistability, driven by the distinct interaction of a degenerate flow-orienting effect and a directed nematic ordering effect, which are not found with rod-like molecules. Uniaxial extensional flow has two characteristic deformations: an extension axis and a plane of uniform compression normal to the extension axis. Discotics subjected to extensional flow attempt to align their unit normals close to the compression plane, that is with $\mathbf{n}$ normal to the extension direction and lying anywhere in the compression plane [9]. In addition, for low nematic potentials (high temperatures) the state of ordering on the compression plane is uniaxial with respect to the extension direction since no preferred direction exists on this (compression) plane. On the other hand, for sufficiently high nematic potentials (low temperatures) a preferred axis is chosen in the compression plane under non-equilibrium flow conditions, such that the ordering has now become biaxial due to the symmetry breaking in this (compression) plane. Since two mutually orthogonal preferred orientation directions on the compression plane can be selected with equal likelihood, both ordering states being equivalent and superposable by a $\pi/2$ rotation, an increase in the extension rate leads to bifurcation phenomena, which according to the magnitude of U turn out to be supercritical (continuous or 2nd order transition), subcritical (discontinuous or 1st order transition), or tricritical (boundary between 1st and 2nd order transitions) transitions involving uniaxial and biaxial phases.

The organization of this paper is as follows. §2 presents the tensor order parameter, the relevant uniaxial and biaxial orientation states, and the Doi equations that govern the dynamics of the scalar order parameters of the disc-like isotropic and liquid crystalline nematic phases in the presence of a uniaxial extensional flow. §3 presents the bifurcation diagram, describes and classifies all the admissible steady states and identifies the multistability regions and critical points in the parameter plane. §4 presents the conclusions of this work.

2. Theory and governing equations

The non-zero components of the symmetric part of the velocity gradient tensor, known as the rate of deformation tensor $\mathbf{A}(A_{ij} = (v_{i,j} + v_{j,i})/2$; $\mathbf{v} \equiv$ velocity), of a steady irrotational uniaxial elongation flow are given by [10]

$$A_{xx} = A_{yy} = -A_{zz}/2 = -\frac{\dot{\varepsilon}}{2}; \ \dot{\varepsilon} > 0 \qquad (1\,a,b)$$

where z is the extension direction, x-y lie on the compression plane, and $\dot{\varepsilon}(\dot{\varepsilon} > 0)$ is the extension rate. The state of order for the discotic nematic liquid crystal is specified by a second order, symmetric and traceless, tensor order parameters $\mathbf{Q}$,

$$\mathbf{Q} \equiv \int f(\mathbf{u})(\mathbf{uu} - \mathbf{I}/3)\mathrm{d}^2\mathbf{u}; \ \mathrm{d}^2\mathbf{u} = \sin\theta\,\mathrm{d}\theta\,\mathrm{d}\phi \qquad (2\,a,b)$$

with the restrictions

$$\int f(\mathbf{u})\mathrm{d}^2\mathbf{u} = 1; \ \mathbf{u}\cdot\mathbf{u} = 1. \qquad (2\,c,d)$$

The symbols $f(\mathbf{u})\mathrm{d}^2\mathbf{u}$ denote the probability of finding a unit molecular normal $\mathbf{u}$ in the solid angle $\mathrm{d}^2\mathbf{u}$, $\mathbf{I}$ is the identity or unit tensor, $\theta(0 \leqslant \theta \leqslant \pi)$ is the polar angle, and $\phi(0 \leqslant \phi \leqslant 2\pi)$ is the azimuthal angle on the unit sphere ($\mathbf{u}\cdot\mathbf{u} = 1$). A widely used parametric representation [11] of $\mathbf{Q}$ in its principal axes is given by

$$\mathbf{Q} = \mu_{\mathbf{n}}\mathbf{nn} + \mu_{\mathbf{m}}\mathbf{mm} + \mu_{\mathbf{l}}\mathbf{ll}, \qquad (3\,a)$$

$$\mu_{\mathbf{n}} = 2S/3, \ \mu_{\mathbf{m}} = (P - S)/3, \ \mu_{\mathbf{l}} = -(P + S)/3 \qquad (3\,b,c,d)$$

and

$$-\tfrac{1}{3} \leqslant \mu_i \leqslant \tfrac{2}{3} \qquad (3e)$$

where $\mathbf{i} = \mathbf{n},\mathbf{m},\mathbf{l}$ are the orthogonal unit eigenvectors, and the $\{\mu_i\}$ are the corresponding eigenvalues. If the three eigenvalues are equal the orientation state is isotropic, if two are equal the state is uniaxial with respect to the direction corresponding to the distinct eigenvalue, and if all three eigenvalues are distinct the state is biaxial. From (3*a*) it follows that the eigenvalues are given by

$$\mathbf{n}\cdot\mathbf{Q}\cdot\mathbf{n} = \mu_\mathbf{n};\ \mathbf{m}\cdot\mathbf{Q}\cdot\mathbf{m} = \mu_\mathbf{m};\ \mathbf{l}\cdot\mathbf{Q}\cdot\mathbf{l} = \mu_\mathbf{l}. \qquad (4a,b,c)$$

Using the definition (2*a*) it also follows that

$$\mathbf{i}\cdot\mathbf{Q}\cdot\mathbf{i} = \mu_i = \int f(\mathbf{u})[(\mathbf{u}\cdot\mathbf{i})^2 - \tfrac{1}{3}]\mathrm{d}^2\mathbf{u};\ \mathbf{i} = \mathbf{n},\mathbf{m},\mathbf{l}. \qquad (5a,b)$$

We next discuss some special cases of interest that follow directly from (3) and (5).

(*a*) Planar Orientation: for $\mu_\mathbf{i} = -\frac{1}{3}$ all the molecular normals (**u**) orient within a plane perpendicular to the **i**th unit vector (i.e. planar orientation). The state of planar orientation for this particularly case ($\mu_\mathbf{i} = -\frac{1}{3}$) can be shown using (5), since when

$$\mathbf{u}\cdot\mathbf{i} = 0 \Leftrightarrow -3\mu_i = \int f(\mathbf{u})\mathrm{d}^2\mathbf{u} = 1;\ \mathbf{i} = \mathbf{n},\mathbf{m},\mathbf{l}. \qquad (6a,b,c)$$

In addition, if the two remaining eigenvalues are equal (distinct) the orientation state is uniaxial (biaxial) and planar.

(*b*) Planar Biaxial Orientation: for $\mu_\mathbf{n} = 0$, $\mu_\mathbf{m} = \frac{1}{3}, \mu_\mathbf{l} = -\frac{1}{3}$ (or $\mu_\mathbf{n} = \frac{1}{3}, \mu_\mathbf{m} = 0, \mu_\mathbf{l} = -\frac{1}{3}$) the state of orientation is planar and biaxial. Here since $\mu_\mathbf{l} = -\frac{1}{3}$ all the unit molecular normals are perpendicular to **l**, and furthermore preferentially distributed along **m**(**n**). For example, for $\mu_\mathbf{n} = 0$ and $\mu_\mathbf{m} = +\frac{1}{3}$, it follows that

$$\int f(\mathbf{u})(\mathbf{u}\cdot\mathbf{m})^2\mathrm{d}^2\mathbf{u} = 2\int f(\mathbf{u})(\mathbf{u}\cdot\mathbf{n})^2\mathrm{d}^2\mathbf{u}. \qquad (7)$$

(*c*) Uniaxial Orientation: for $\mu_\mathbf{n} = \mu_\mathbf{m}$ the ordering is uniaxial with respect to **l**.

To specify the molecular geometry we approximate the disc-like shape with an oblate spheroid of aspect ratio $p = R_\parallel R_\perp$ ($p < 1$), where $R_\parallel$ is the length of the shortest and distinct semiaxis, and $R_\perp$ the length of the two longest and equal semiaxes. The ideal flat disc corresponds to $p = 0$, and the sphere corresponds to $p = 1$. In a polydisperse material, we should use a distribution function for p, while for the monodisperse assumption adopted here p is unique.

Using Doi's mesoscopic nematodynamic theory [12] the dynamic equation for the tensor order parameter **Q** in the presence of an irrotational flow is found to be

$$\frac{\mathrm{d}\mathbf{Q}}{\mathrm{d}t} = \tfrac{2}{3}\beta\mathbf{A} + \beta[\mathbf{A}\cdot\mathbf{Q} + \mathbf{Q}\cdot\mathbf{A} - \tfrac{2}{3}(\mathbf{A}:\mathbf{Q})\boldsymbol{\delta}] - 2\beta(\mathbf{A}:\mathbf{Q})\mathbf{Q} - 6D\left\{\left(1 - \frac{U}{3}\right)\mathbf{Q} - U\mathbf{Q}\cdot\mathbf{Q} + U[(\mathbf{Q}:\mathbf{Q})\mathbf{Q} + \tfrac{1}{3}(\mathbf{Q}:\mathbf{Q})\boldsymbol{\delta}]\right\} \qquad (8)$$

where $\beta = (p^2 - 1)/(p^2 + 1)$, D is the diffusivity, $U = 3T^*/T$ is the nematic potential, T is the temperature, and T^* is the temperature below which the isotropic phase becomes unstable. Since the flow is irrotational we neglected the vorticity contribution to (8). In addition the shape factor β now appears in all the flow contributions. It is worth noting that previous work using similar versions of the Doi equation were aimed at describing the rheology of rigid rod-like polymers, in which case $p \to +\infty$ and $\beta = 1$. The first three terms on the right hand side of equation (8) correspond to the flow contribution and the rest to the thermodynamic effect, which is a special two parameter form of the four parameter expression derived from the Landau–de Gennes free energy [12]. Derivation of equation (8) uses the decoupling approximation [12], which in the absence of vorticity will only affect the accuracy but not the nature of the solutions. Here we also assume for simplicity that D is constant. For steady uniaxial extensional flow of discotic nematics or paranematics, the eignenvector **l** aligns in the extension (**z**) direction, and the diad (**n**, **m**) aligns anywhere in the compression plane. Thus we write equation (8) in the principal axes of **Q**, and consider the following equations motions for the two scalar order parameters:

$$\frac{\mathrm{d}S}{\mathrm{d}t} = -\frac{P_\mathrm{e}}{2}\{(1 + 2S)(P + S - 1)\} - \left\{\left(1 - \frac{U}{3}\right)S - \tfrac{2}{3}US^2 + \frac{U}{9}(3S^2 + P^2)(1 + 2S)\right\} \qquad (9)$$

and

$$\frac{\mathrm{d}P}{\mathrm{d}t} = -P_\mathrm{e}\{-\tfrac{3}{2} + S + (P + S)(\tfrac{1}{2} + P)\} - \left\{\left(1 - \frac{U}{3}\right)P + \frac{U}{3}(3S^2 + P^2 + 2PS) - \tfrac{2}{3}U(3S^2 + P^2)\left(\frac{1}{2} - \frac{P}{3}\right)\right\} \qquad (10)$$

where P_e is the Peclet number given by $P_\mathrm{e} = \dot{\varepsilon}|\beta|/6D$, and t is now scaled with D.

Table 1. Nomenclature, symmetry, and characterization of stable stationary solutions.

Solution symbol	Solution symmetry	Sign of S	Sign of P	Sign of $\mu_{\mathbf{n}} = 2S/3$	Sign of $\mu_{\mathbf{m}} = (P-S)/3$	Sign of $\mu_{\mathbf{l}} = -(P+S)/3$	Eigenvalue ordering
PN	Uniaxial paranematic	+	+	+	+	−	$\mu_n = \mu_m > \mu_l$
B^{++}	Biaxial nematic	+	+	+	+	−	$\mu_n > \mu_m > \mu_l$ and $\mu_m > \mu_n > \mu_l$
B^{-+}	Biaxial nematic	−	+	−	+	−	$\mu_m > \mu_n > \mu_l$
N^{--}	Uniaxial nematic	−	−	−	−	+	$\mu_l > \mu_n = \mu_m$

3. Results and discussion

Equations (9)–(10) describe a planar (P, S) two parameter (U, P_e) non-linear dynamical system. Bifurcational and phase plane analysis of equations (9)–(10) were performed using standard procedures for non-linear dynamical systems [13].

Table 1 characterizes the four classes of steady state solutions to equations (9)–(10) using the signs of the scalar order parameters (or eigenvalues), and the ordering of the eigenvalues of $\mathbf{Q}$. These four steady state solutions to equations (9)–(10) are

Steady State Solutions:
- PN: Uniaxial paranematic
- B^{++}: Biaxial nematic
- B^{-+}: Biaxial nematic
- N^{++}: Uniaxial nematic

where the superscripts refer to the corresponding signs of S and P, respectively. As discussed in detail below, the two biaxial nematic solutions represent physically and dissipatively identical solutions.

The paranematic (PN) phase, obtained by subjecting the isotropic phase to the uniaxial extension, is uniaxial ($\mu_{\mathbf{n}} = \mu_{\mathbf{m}}$) with respect to the extension direction (eigenvector $\mathbf{l}$). The paranematic phase is an isotropic phase and is not a nematic liquid crystalline phase. The type of flow-induced ordering displayed by the PN phase is characteristic of isotropic fluids composed of orientable molecules of molecular segments, such as solutions of flexible polymers. The important characteristics of the orientation are

$$P = 3S;\ \mu_{\mathbf{n}} = \mu_{\mathbf{m}} = 2S/3;\ \mu_{\mathbf{l}} = -4S/3. \qquad (11\,a,b,c)$$

The nematic biaxial B^{++} phase, with $S > 0$ and $P > 0$, may have preferential alignment along $\mathbf{n}$ ($\mu_{\mathbf{n}} > \mu_{\mathbf{m}}$) or along $\mathbf{m}$ ($\mu_{\mathbf{m}} > \mu_{\mathbf{n}}$). The nematic biaxial B^{-+} phase, with $S < 0$ and $P > 0$, has a higher molecular alignment along $\mathbf{m}$ than along $\mathbf{n}$ ($\mu_{\mathbf{m}} > \mu_{\mathbf{n}}$). These two biaxial nematic phases are physically and dissipatively equivalent: a $\pi/2$ rotation along the extension axis turns the B^{++} solution into the B^{-+} solution. This equivalence is reflected in the following eigenvalues identities:

$$\mu_{\mathbf{n}}(B^{-+}) = \mu_{\mathbf{m}}(B^{-+}), \qquad (12\,a)$$

$$\mu_{\mathbf{m}}(B^{++}) = \mu_{\mathbf{n}}(B^{-+}), \qquad (12\,b)$$

and

$$\mu_{\mathbf{l}}(B^{++}) = \mu_{\mathbf{l}}(B^{-+}). \qquad (12\,c)$$

In words, a $\pi/2$ rotation around the extension axis of the tensor ellipsoid corresponding to the B^{++} superposes with the unrotated tensor ellipsoid of the B^{-+} solution. This equivalence follows naturally from the uniform compression field acting in the $\mathbf{n} - \mathbf{m}$ plane. A bias in the compression $(\mathbf{n} - \mathbf{m})$ plane will invalidate the identities given in (12). As shown in table 1, two biaxial B^{++} phases may be present, with the only difference that the roles of $\mathbf{n}$ and $\mathbf{m}$ are again switched. The only difference of this case with the previous one is that both S and P are positive in both solutions. To differentiate these two biaxial phases we use B_1^{++} and B_2^{++}, where the subscript identifies the solution. When two B^{++} phases exist we find

$$\mu_{\mathbf{n}}(B_1^{++}) = \mu_{\mathbf{m}}(B_2^{++}), \qquad (13\,a)$$

$$\mu_{\mathbf{m}}(B_1^{++}) = \mu_{\mathbf{n}}(B_2^{++}), \qquad (13\,b)$$

and

$$\mu_{\mathbf{l}}(B_1^{++}) = \mu_{\mathbf{l}}(B_2^{++}). \qquad (13\,c)$$

Again the B_1^{++} and B_2^{++} are physically and dissipatively equivalent. For the biaxial nematic phases we always have $P \neq 3S$, since then all eigenvalues are distinct. The physical reason why these biaxial phases occur is due to the degenerate nature of the compression plane and the focusing effect of the nematic orientation field. In more detail, the main direction of alignment is in the com-

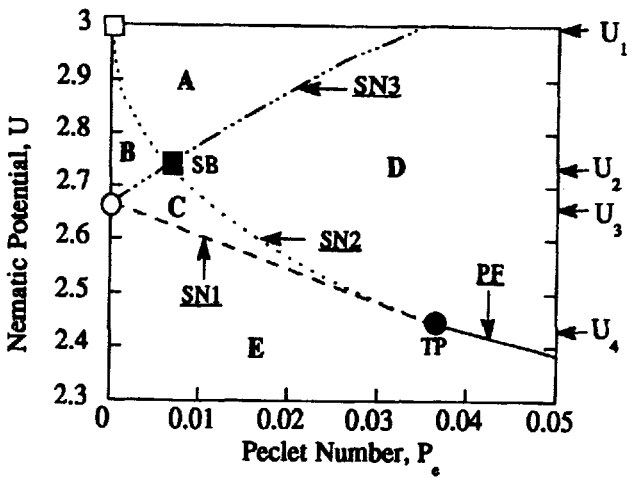

Figure 2. Computed bifurcation diagram of equations (4)–(6) in terms of the nematic potential (U) and the Peclet number (P_e). The stable solutions in each of the five regions are characterized in tables 1 and 2. The four different lines represent four different bifurcations (see text). The births and intersections of the four bifurcations lines are indicated by filled and unfilled squares and circles, and their parametric location and meanings are summarized in table 3.

pression plane (flow effect) and the type of deformations on the plane normal to the selected main director (thermodynamic effect) is therefore non-uniform. The plane normal to the main director passes through the x axis. The non-uniform deformations in the plane normal to the main director contain compressions (for example, along the compression y-z plane) and extensions (for example, along the extension axis). Thus on a plane normal to the main director the deformations are different and the nematic phase must then be biaxial.

The N^{--} phase ($\mu_n = \mu_m$), with $S<0$ and $P<0$, is a uniaxial nematic phase. It is stable only at low extension rates since it favours molecular alignment along the extension direction. This uncommon nematic phase appears since in the absence of flow, the model predicts the existence of the abnormal ($S<0, P<0$) nematic phase; a similar situation appears in purely uniaxial phases [1, 11]. Increasing the flow strength just tend to decrease the molecular alignment along the extension direction, until it becomes unstable at a certain critical extension rate. We note that as shown below the N^{--} and the PN phases coexist in a certain range of extension rates (P_e) and temperatures (U). The important characteristics of the orientation are again given by (11) and the only difference arises from the signs of S ($S<0$) and P ($P<0$).

Figure 2 shows the bifurcation diagram in terms of U and P_e. The four different lines on the plane denote the following standard [13] bifurcation phenomena: (*a*) SN1: saddle-node bifurcation denoting the stability exchange of the two equivalent biaxial nematic B^{++} and B^{-+} solutions; (*b*) SN2: saddle-node bifurcation denoting the stability exchange of the uniaxial paranematic solution; (*c*) SN3: saddle-node bifurcation denoting the stability exchange of the uniaxial U^{--} solution; (*d*) PF: pitchfork bifurcation of the uniaxial PN phase into two biaxial nematic B^{++} solutions. The SN1 and SN2 pair represent a subcritical bifurcation, involving the PN, B^{-+}, and B^{++} solutions. The four bifurcation lines divide the U-P_e plane into five regions; the stable solutions and parametric conditions in each region are enumerated in table 2, where the subscripts in the parameters of the first two columns refer to a bifurcation line. Region E is the only region without multistability. We note that the values $U_{SN1}, U_{SN2}, U_{SN3}, U_{PF}$ appearing in table 2 are functions of P_e; the functionality can be read off figure 2.

The birth, crossing, and intersections of the four bifurcation lines are identified in figure 2 by open and filled squares and circles, and their meanings and parametric conditions are enumerated in table 3. The merging of two saddle node bifurcations (SN1 and SN2), denoting a discontinuous subcritical bifurcation (1st order transition), with the pitchfork bifurcation (2nd order transition) line results in the tricritical point indicated by a filled circle in figure 2.

Next we discuss the solution behaviour observed by increasing P_e from zero at different but constant nematic potentials. For $U > U_1$ the stable phases are nematic, and when crossing the SN3 line the uniaxial N^{--} branch, exhibiting preferred alignment towards the extension direction, becomes unstable; the stable N^{--} branch is not connected to any other stable branch. For $U_2 < U < U_1$, a sufficient increase in P_e first results in the subcritical bifurcation at SN2 of the uniaxial PN branch into the two

Table 2. Multistability regions of bifurcation diagram.

Peclet number $P_e = \dot{\varepsilon}\lvert\beta\rvert/6D$	Nematic potential $U = 3T^*/T$	Region in bifurcation diagram	Linearly stable solutions
$P_e > 0$	$U > U_{SN2}$ $U > U_{SN3}$	A	N^{--}, B^{-+}, B^{++}
$0 < P_e < P_{eSB}$†	$U_{SN3} < U < U_{SN2}$	B	PN, N^{--} B^{-+}, B^{++}
$0 < P_e < P_{eTP}$‡	$U_{SN1} < U < U_{SN2}$ $U < U_{SN3}$	C	PN, B^{-+}, B^{++}
$P_{eSB} < P_e$	$U_{SN2} < U < U_{SN3}$	D	B^{-+}, B^{++}
$0 < P_e$	$U < U_{SN1}$ $U < U_{PF}$	E	PN

‡ $P_{eTP} \approx 0{\cdot}0351$.
† $P_{eSB} \approx 0{\cdot}007$.

Table 3. Transition and critical points in bifurcation diagram.

Peclet number $P_e = \dot{\varepsilon}\lvert\beta\rvert/6D$	Nematic potential $U = 3T^*/T$	Symbol	Bifurcation/transition/stability
$P_e = 0$	$U_1 = 3$	□	Birth of SN2: PN becomes unstable
$P_e \approx 0{\cdot}007$	$U_2 \approx 2{\cdot}73$	■	Simultaneous saddle-node bifurcations (SB): SN2 and SN3
$P_e = 0$	$U_3 = 8/3$	○	Birth of SN3: N^{--} exchanges stability Birth of SN1: B^{-+} and B^{++} exchange stability
$P_e \approx 0{\cdot}0351$	$U_4 \approx 2{\cdot}45$	●	Tricritical point (TP): merging of saddle-node (SN1, SN2) and pitchfork bifurcations (PF)
$P_e \to \infty$	$U_5 \approx 1{\cdot}382$	—	For $U < U_5$, PN is stable

biaxial nematic B^{-+} and B^{++} branches, and then at SN3 in the loss of stability of the uniaxial N^{--} branch. For $U_3 < U < U_2$, an increase in P_e first results in the loss of stability of N^{--}, and at higher P_e in the subcritical bifurcation of the PN branch into the B^{-+} and B^{++} branches. For $U_4 < U < U_3$, an increase in P_e results in the subcritical bifurcation of the PN branch into the B^{-+} and B^{++} branches. For $U_5 < U < U_4$, a sufficient increase in P_e results in the pitchfork bifurcation of the uniaxial PN branch into two biaxial B^{++} branches. Finally, for $U < U_5$, the paranematic phase remains stable at all P_e, and as $P_e \to \infty$ the molecular orientation is normal to the extension direction and uniaxial.

Next we identify and use a validation procedure to ensure the general validity of the present results. A significant issue allowing for the validation of the present solution multistabilities and tricritical point, as shown in figure 2, emerges by considering the biaxial extensional flow of rigid rod-like nematic polymers. As mentioned above, for rigid rod polymers the characteristic shape factor is $\beta = 1$. For biaxial extensional flow [13] the non-zero components of the rate of deformation tensor (**A**) now are

$$A_{xx} = A_{yy} = -A_{zz}/2 = -\frac{\dot{\varepsilon}}{2};\ \dot{\varepsilon} > 0 \qquad (14\,a,b)$$

where z is now the compression axes, the x-y plane is now the extension plane, and the extension rate is now negative, $\dot{\varepsilon} < 0$ (compare with equation (1)). The governing equation (8) shows that the rate of deformation tensor **A** is always multiplied by the shape factor β, and therefore a simultaneous sign change in both **A** and β leaves the Doi equation of nematodynamics invariant. Thus we can conclude that the biaxial extensional flow of rigid rod nematics is equivalent to the uniaxial extensional flow of discotic nematics. Therefore the multistability and tricriticality predicted in the present paper should also hold for rod-like nematic liquid crystals in the presence of biaxial extensional flow. This conclusion is essentially confirmed by comparing figure 2 with the predictions of Khoklov and Semenov on biaxial extensional flow of rigid rod nematic polymers, using the Onsager model and the dynamical free energy method [14]. Comparison of our figure 2 with figure 7 of reference [14] shows exactly the same multistability behaviour and tricriticality; the only minor difference in the two bifurcation diagrams is that in reference [14] the abnormal uniaxial nematic phase N^{--} is not predicted. Although the present results have not been validated by experiments due to lack of data, the remarkable agreement found with [14] (who used a different theory and a different solution method) provides strong evidence of the general validity of the present predictions.

In partial summary, the Doi equation of nematodynamics adapted to discotics in the presence of uniaxial extensional flow admits four steady states. In the temperature (U) extension rate (P_e) phase diagram, a rich multistability behaviour and tricriticality is predicted. This is in stark contrast to the predictions of rod-like nematics in uniaxial extensional flow [6, 8], where the only phases present are all uniaxial and where tricriticality is therefore absent. In the present paper tricriticality must be present because the isotropic (PN) phase is uniaxial while the normal nematic (B^{++} or B^{-+}) phase is biaxial, and thus even at infinite extension rates a decrease in temperature will result in a non-equilibrium uniaxial-to-biaxial second order phase transition (i.e. PN $\Rightarrow$ B). Since fibre manufacturing from rod-like (such as Kevlar) and disc-like (such as mesophase carbon fibre) nematics involves uniaxial extensional flow, and as shown here the two flows are drastically different, we can conclude that the microstructural phenomena during fibre formation will be strongly different. A similar conclusion for seemingly different reasons was also reached by de Gennes [15].

4. Conclusions

In summary, we have presented and discussed the bifurcation diagram in the reduced temperature and extension rate plan, of the non-equilibrium isotropic–discotic nematic phase transition in the presence of extensional flow. A characterization of molecular ordering of the stable stationary solutions to Doi's equation of nematodynamics, specialized to disc-like materials, has been presented. The source of the rich phenomenology, not found for rod-like nematics, of multiple steady uniaxial and biaxial states in extensional flow is found to be the interaction between the degenerate flow-induced orientation of disc-like molecules away from the extension direction, and the selection, at higher nematic potential, of a pair of equivalent preferential orientation axes. Finally, a tricritical non-equilibrium phase transition point has been identified. It is expected that all these findings may be used to increase the current understanding of the spinning of carbon fibres using biphasic isotropic–discotic nematic precursors [3], and the rheology of discotic nematic liquid crystals in general. Although the predictions were not validated with experimental data, an evaluation procedure using the equivalence between the extensional flow of discotic nematics and the biaxial extensional flow of rod-like nematics was identified and used. The present results predicted by the Doi model are essentially identical to those obtained in [14] for the equivalent biaxial extensional flow of rigid rod-like nematic polymers, using the Onsager theory and the dynamical free energy method.

This work is supported by the Natural Science and Engineering Research Council of Canada (NSERC).

References

[1] DE GENNES, P. G., and PROST, J., 1993, *The Physics of Liquid Crystals*, 2nd edition (Clarendon Press).
[2] CHANDRASEKHAR, S., 1992, *Liquid Crystals*, 2nd edition (Cambridge University Press).
[3] GASPAROUX, H., 1981, *Molec. Crystals liq. Crystals*, **63,** 231.
[4] OLMSTEAD, P. D., and GOLDBART, P., 1990, *Phys. Rev.* A, **41,** 4578.
[5] WANG, C., VUGMEITER, B. E., and OU-YANG, H. D., 1993, *Phys. Rev.* E, **48,** 4455.
[6] SEE, H., DOI, M., and LARSON, R. G., 1990, *J. chem. Phys.*, **92,** 792.
[7] LEE, S. D., 1987, *J. chem. Phys.*, **86,** 6567.
[8] HU, T. D., and RISKIN, G., 1992, *J. chem. Phys.*, **96,** 4705.
[9] SINGH, A. P., and REY, A. D., 1994, *J. Phys. II*, **4,** 645.
[10] BIRD, R. B., CURTISS, C. F., ARMSTRONG, R. G., and HASSAGER, O., 1987, *Dynamics of Polymeric Liquids*, Vol. 1 (Wiley, New York).
[11] VERTOGEN, G., and DE JEU, W. H., 1988, *Thermotropic Liquid Crystals: Fundamentals* (Springer-Verlag), p. 224.
[12] DOI, M., and EDWARDS, S. F., 1986, *The Theory of Polymer Dynamics* (Clarendon Press), p. 358.
[13] HALE, J., and KOCAK, H., 1991, *Dynamics and Bifurcation* (Springer-Verlag), p. 170.
[14] KHOKHLOV, A. R., and SEMENOV, A. N., 1982, *Macromolecules*, **15,** 1272.
[15] DE GENNES, P. G., 1982, *Polymer Liquid Crystals*, edited by A. Ciferri, W. R. Krigbaum, and R. B. Meyer (Academic Press), p. 118.